Naval Research Laboratory

Washington, DC 20375-5320

Analysis and Simulations of Optical Rectification as a Source of Terahertz Radiation

D. F. Gordon
P. Sprangle

Beam Physics Branch
Plasma Physics Division

C. A. Kapetanakos

Leading Edge Technologies Corporation
Washington, DC

August 15, 2005

REPORT DOCUMENTATION PAGE

1. REPORT DATE (DD-MM-YYYY) 15-08-2005	2. REPORT TYPE Memorandum Report	3. DATES COVERED (From - To) November 30, 2003-November 30, 2004

4. TITLE AND SUBTITLE

Analysis and Simulations of Optical Rectification as a Source of Terahertz Radiation

5a. CONTRACT NUMBER

5b. GRANT NUMBER

5c. PROGRAM ELEMENT NUMBER

6. AUTHOR(S)

D.F. Gordon, P. Sprangle, and C.A. Kapetanakos*

5d. PROJECT NUMBER
67-8833-05

5e. TASK NUMBER

5f. WORK UNIT NUMBER

7. PERFORMING ORGANIZATION NAME(S) AND ADDRESS(ES)

Naval Research Laboratory, Code 6791
4555 Overlook Avenue, SW
Washington, DC 20375-5320

8. PERFORMING ORGANIZATION REPORT NUMBER

NRL/MR/6791--05-8869

9. SPONSORING / MONITORING AGENCY NAME(S) AND ADDRESS(ES)

Office of Naval Research
800 North Quincy Street
Arlington, VA 22217

10. SPONSOR / MONITOR'S ACRONYM(S)

ONR

11. SPONSOR / MONITOR'S REPORT NUMBER(S)

12. DISTRIBUTION / AVAILABILITY STATEMENT

Approved for public release; distribution is unlimited.

13. SUPPLEMENTARY NOTES

*Leading Edge Technologies (LET) Corporation, 4431 MacArthur Blvd., Washington, DC 20007

14. ABSTRACT

The second order nonlinearity present in many crystals can be utilized to convert optical radiation into THz radiation via the optical rectification mechanism. This process becomes efficient if a phase matching condition is satisfied. The short pulses used for optical rectification can be more intense than the longer pulses used for difference frequency generation because of the pulse length dependence of the crystal's damage threshold. However, optical rectification is more complicated than difference frequency generation because of the fact that the THz is broadband and group velocity dispersion cannot be neglected. Simulations show that conversion efficiencies of one percent can be obtained from optical rectification in a Gallium Selenide crystal, provided a means of coupling the radiation into and out of the crystal can be found. The saturation of the THz signal is due to frequency shifts in the laser pulse, which change the group velocity and spoil the phase matching. As part of the process, the laser pulse is dramatically compressed.

15. SUBJECT TERMS

Terahertz radiation; Down conversion; Nonlinear optics; Optical Rectification

16. SECURITY CLASSIFICATION OF:			17. LIMITATION OF ABSTRACT	18. NUMBER OF PAGES	19a. NAME OF RESPONSIBLE PERSON Daniel F. Gordon
a. REPORT Unclassified	b. ABSTRACT Unclassified	c. THIS PAGE Unclassified	UL	34	19b. TELEPHONE NUMBER (include area code) (202) 767-5036

This page intentionally blank.

Contents

ANALYSIS AND SIMULATIONS OF OPTICAL RECTIFICATION AS A SOURCE OF TERAHERTZ RADIATION

I.   INTRODUCTION

Diode pumped laser systems based on chirped pulse amplification [1] are capable of delivering millijoule sub-picosecond pulses at repetition rates as high as 10 kilohertz. These compact and efficient lasers can be used to generate high average power terahertz (THz) radiation if an efficient photonic downconversion scheme can be found.

Photonic downconversion is a set of methods whereby optical or infrared radiation is converted to a lower frequency due to the effects of the second order susceptibility present in anisotropic materials. With an appropriate pump source and nonlinear medium these methods can be used to generate THz radiation [2, 3, 4, 5, 6, 7, 8, 9, 10, 11]. The conversion efficiency achieved by these methods scales with several parameters, including the pump intensity, the interaction length, the absorption losses, the nonlinearity, and the phase mismatch.

Ultimately, achieving breakthrough conversion efficiencies cannot be achieved simply by tuning parameters such as laser power or interaction length. In fact, in the regime where many experiments operate, the conversion efficiency is fundamentally limited by the Manley-Rowe relation to a value given by

$$\eta_{MR} = \frac{\lambda_p}{\lambda_s} \tag{1}$$

where λ_s is the wavelength of the signal being generated and λ_p is the wavelength of the pumping radiation. In the case of Ref. [9], for example, $\lambda_p = 1.06$ μm and $\lambda_s = 300$ μm so that $\eta_{MR} = 0.33\%$. This low value can only be exceeded by designing a system which operates in a regime where the assumptions of the Manley-Rowe relation do not hold. One such assumption is that the radiation consists of three discrete frequencies. By operating in a regime where the bandwidth of the pump radiation is comparable to the signal frequency, it may be possible to obtain conversion efficiencies exceeding η_{MR}.

In this report we consider utilizing ultra-short laser pulses to efficiently generate THz radiation via a phase matched optical rectification process. Optical rectification generates radiation with a center frequency approximately equal to the inverse of the pulse length of the pump laser. If the spot size of the laser is many THz wavelengths in diameter, the process can be phase matched by angle tuning in a suitable crystal.

II. TECHNICAL BACKGROUND

A. Normalizations

We use a system of units normalized as follows. The unit of time is ω_T^{-1} where $\omega_T = 2\pi \times 10^{12}$ rad/s. The unit of length is c/ω_T, where c is the speed of light. The unit of mass is the electronic mass, m, and the unit of charge is the electronic charge, $|e|$. The unit of density is $n_T = m\omega_T^2/4\pi e^2$. Note that this results in the peculiarity that the unit of particle number is $N_T = mc^3/4\pi\omega_T e^2$. To determine the value of a normalized quantity in either SI or gaussian units, multiply the normalized quantity by the value given in Table I. For the case of SI units, we define the permittivity of free space, $\epsilon_0 = 8.85 \times 10^{-12}$ F/m, and the impedance of free space, $\eta_0 = 377\ \Omega$.

B. Coordinate System

Two natural coordinate systems arise when considering laser propagation in a crystal. In one coordinate system the description of the interaction with the crystal is simplified, while in the other the description of the laser propagation is simplified. The former will be described by the "crystal basis" defined by the unit vectors $(\mathbf{u}, \mathbf{v}, \mathbf{w})$. The latter will be described by the "laser basis" defined by the unit vectors $(\mathbf{x}, \mathbf{y}, \mathbf{z})$. We will consider the laser basis to coincide with the standard basis.

In a general coordinate system, the linear response of the electronic polarization $\mathbf{P}$ to an applied field $\mathbf{E}$ is given by the tensor equation $P_i = \chi_{ij}E_j$ (we use the Einstein summation convention). By definition, χ_{ij} is diagonal in the crystal basis. Furthermore, for uniaxial crystals two of the diagonal elements are equal. By convention the two equal elements are $\chi_{uu} = \chi_{vv}$. In this case, radiation with a polarization component in the $\mathbf{w}$ direction is called an extraordinary wave, while radiation with no polarization components in the $\mathbf{w}$ direction is called an ordinary wave.

The laser basis is defined such that the central wavevector of the laser points in the $\mathbf{z}$ direction. The orientations of $\mathbf{x}$ and $\mathbf{y}$ with respect to the laser polarization can only be made meaningful after specifying the relation between the laser basis and the crystal basis.

TABLE I: Normalization

Quantity	Symbol	SI Unit	cgs Unit	Unit Value
Time		ω_T^{-1}	ω_T^{-1}	159 fs
Length		c/ω_T	c/ω_T	47.8 μm
Density	n_T	$\epsilon_0 m\omega_T^2/e^2$	$m\omega_T^2/4\pi e^2$	1.24×10^{16} cm^{-3}
Particle Number		$\epsilon_0 mc^3/\omega_T e^2$	$mc^3/4\pi\omega_T e^2$	1.35×10^9
Electric Field	E_T	$mc\omega_T/e$	$mc\omega_T/e$	107 MV/cm
Magnetic Field		$m\omega_T/e$	$mc\omega_T/e$	35.7 T
Current Density		$n_T ec$	$n_T ec$	59.5 A/cm^2
Charge Density		$n_T e$	$n_T e$	0.0020 C/cm^3
Polarization		$n_T ec/\omega_T$	$n_T ec/\omega_T$	9.5×10^{-8} C/m^2
Susceptibility^a		1	$1/4\pi$	
Susceptibility (2$^{\text{nd}}$ order)		$1/E_T$	$1/4\pi E_T$	9.3×10^{-11} m/V
Susceptibility (3$^{\text{rd}}$ order)		$1/E_T^2$	$1/4\pi E_T^2$	8.7×10^{-21} m^2/V^2
Energy		mc^2	mc^2	8.19×10^{-14} J
Energy Density		$mc^2 n_T$	$mc^2 n_T$	1.02 kJ/cm^3
Power		$mc^2\omega_T$	$mc^2\omega_T$	0.52 W
Fluence		$E_T^2/\eta_0\omega_T$	$cE_T^2/4\pi\omega_T$	4.83 J/cm^2
Intensity	I_T	E_T^2/η_0	$cE_T^2/4\pi$	3.04×10^{13} W/cm^2
Two Photon Coefficient		ω_T/cI_T	ω_T/cI_T	0.0069 cm/GW

^{a}For the SI units, we use the convention whereby ϵ_0 is not absorbed into the susceptibility; i.e., $P = \epsilon_0 \chi E$.

The laser basis and the crystal basis are connected by a rotation operator

$$T = R_y(-\theta)R_z(-\phi) \tag{2}$$

where R_y and R_z represent right-handed rotations about the y and z axes. Written out explicitly,

$$T = \begin{pmatrix} \cos\theta\cos\phi & -\cos\theta\sin\phi & -\sin\theta \\ \sin\phi & \cos\phi & 0 \\ \sin\theta\cos\phi & -\sin\theta\sin\phi & \cos\theta \end{pmatrix} \tag{3}$$

Physically, the operator T corresponds to the following procedure. Position the crystal such that the crystal basis coincides with the laser basis. Rotate the crystal $-\phi$ about the z axis, then rotate it $-\theta$ about the y axis. With this procedure, waves polarized in the x-direction are extraordinary waves while waves polarized in the y-direction are ordinary waves.

Mathematically, the operator T takes a vector expressed in the crystal basis and gives the same vector expressed in the laser basis:

$$\mathbf{A}_{LB} = T\mathbf{A}_{CB} \tag{4}$$

Here, the subscript CB refers to the crystal basis and the subscript LB refers to the laser basis. If the basis vectors themselves are expressed in the standard basis , they satisfy

$$(\mathbf{u}, \mathbf{v}, \mathbf{w}) = T(\mathbf{x}, \mathbf{y}, \mathbf{z}) \tag{5}$$

An operator $\hat{L}$ is transformed according to

$$\hat{L}_{LB} = T\hat{L}_{CB}T^{-1} \tag{6}$$

Because T is an orthogonal matrix, its inverse can be computed simply by taking the transpose

$$T^{-1} = T^T \tag{7}$$

C.   Timescale Separation and Laser Frame

Numerical models of optical rectification can be made more efficient by taking advantage of the large time-scale separation between the laser frequency and the THz frequency. This is done by averaging over the fast laser oscillations, but not the much slower THz oscillations. Let the real valued laser field be denoted $\tilde{\mathcal{E}}_i$ and the real valued THz field by E_i. The complex amplitude of the laser field, $\mathcal{E}_i$, is then defined by

$$\tilde{\mathcal{E}}_i = \frac{\mathcal{E}_i}{2}e^{i(\omega_0 t - k_0 z)} + c.c. \tag{8}$$

The demand on computing resources can be minimized by solving only for the complex envelope $\mathcal{E}_i$ which varies much more slowly than the real valued field $\tilde{\mathcal{E}}_i$. A similar notation will be used for all other quantities. For example, the electronic polarization is similarly decomposed into the rapidly varying part, denoted by the real valued $\tilde{\mathcal{P}}_i$ and complex valued $\mathcal{P}_i$, and the slowly varying part, denoted by P_i.

Further computational advantage can be gained by carrying out the calculations in a Galilean frame of reference moving at the group velocity of the laser pulse. In this frame of reference, the independent variables become $\eta = z$ and $\tau = t - n_g z$. The corresponding differential operators transform according to

$$\partial_z = \partial_\eta - n_g \partial_\tau \tag{9}$$

$$\partial_t = \partial_\tau \tag{10}$$

The group index, often called β_1, is given by

$$n_g = n(\omega_0) + \omega_0 \left.\frac{dn}{d\omega}\right|_{\omega=\omega_0} \tag{11}$$

The utility of this coordinate system arises from the fact that for short pulses propagating in the forward direction $\partial_\eta \ll \partial_\tau$. By dropping terms containing ∂_η^2 from the propagation equations one obtains equations that can be integrated without the restrictive Courant condition that would otherwise apply.

D. Boundary Conditions

When a light pulse enters a dielectric the spatial length of the pulse and the relative strength of the electric and magnetic fields are changed. Suppose the dielectric is anti-reflection coated. Then the energy in the dielectric can be equated with the energy in the vacuum. The energy of the pulse in vacuum is

$$U_v = \int E_v^2 dV \tag{12}$$

where we used $E_v = B_v$, dV is a volume element, and the integral is over all space. The energy in the dielectric is

$$U_d = \frac{1}{2} \int \left(E_d^2 + B_d^2 + \mathbf{E}_d \cdot \mathbf{P} \right) dV \tag{13}$$

It is easy to show using Maxwell's equations that if the index of refraction is n_o, then

$$|B_d| = n_o |E_d| \tag{14}$$

Using $P = (n_o^2 - 1)E_d$ then gives

$$U_d = \int n_o^2 E_d^2 dV \tag{15}$$

By equating U_d and U_v, and taking into account that in the dielectric the pulse is spatially compressed by a factor n_o, we conclude that

$$E_v^2 = n_o E_d^2 \tag{16}$$

$$B_v^2 = \frac{B_d^2}{n_o} \tag{17}$$

It follows that the Poynting vector $\mathbf{E} \times \mathbf{B}$ is conserved as the pulse passes from vacuum into the dielectric. By expanding the Poynting vector we obtain a formula for the average intensity in the dielectric:

$$\langle I \rangle = \frac{n_o |\mathcal{E}_d|^2}{2} \tag{18}$$

Here $\mathcal{E}_d$ is the complex envelope described above. It should be noted that this intensity takes into account the movement of the energy associated with the material's dipole moment. The rate of power flow associated with the fields only is given by

$$\langle I_{\text{field}} \rangle = \frac{(1 + n_o^2)|\mathcal{E}_d|^2}{4n_o} \tag{19}$$

E. Dispersionless Linear Propagation in a Uniaxial Crystal

Suppose the linear susceptibility tensor in the crystal basis is given as

$$\chi_{CB} = \begin{pmatrix} \chi_o & 0 & 0 \\ 0 & \chi_o & 0 \\ 0 & 0 & \chi_e \end{pmatrix} \tag{20}$$

Then Eq. (6) gives it in the laser basis as

$$\chi_{LB} = \begin{pmatrix} \chi_{11} & 0 & \chi_c \\ 0 & \chi_o & 0 \\ \chi_c & 0 & \chi_{33} \end{pmatrix} \tag{21}$$

where

$$\chi_{11} = \chi_o \cos^2\theta + \chi_e \sin^2\theta \tag{22}$$

$$\chi_c = (\chi_o - \chi_e)\cos\theta \sin\theta \tag{23}$$

$$\chi_{33} = \chi_e \cos^2\theta + \chi_o \sin^2\theta \tag{24}$$

Note that there is no dependence on ϕ, as expected for a uniaxial crystal. The exact wave equation for the electric field in a perfect insulator is

$$\left(\nabla^2 - \partial_t^2\right) \mathbf{E} = \partial_t^2 \mathbf{P} + \nabla\left(\nabla \cdot \mathbf{E}\right) \tag{25}$$

Note that in an anisotropic medium the divergence term cannot be neglected. Taking the one dimensional limit, and using $P_i = \chi_{ij} E_j$, we obtain three equations in three unknowns:

$$\left(\partial_z^2 - \partial_t^2\right) E_x = \partial_t^2 \left(\chi_{11} E_x + \chi_c E_z\right) \tag{26}$$

$$\left(\partial_z^2 - \partial_t^2\right) E_y = \chi_o \partial_t^2 E_y \tag{27}$$

$$- \partial_t^2 E_z = \partial_t^2 \left(\chi_c E_x + \chi_{33} E_z\right) \tag{28}$$

The equation for E_z can be solved immediately giving

$$E_z = -\frac{\chi_c}{1 + \chi_{33}} E_x \tag{29}$$

This results in two independent propagation equations for the transverse components:

$$\left(\partial_z^2 - n_\theta^2 \partial_t^2\right) E_x = 0 \tag{30}$$

$$\left(\partial_z^2 - n_o^2 \partial_t^2\right) E_y = 0 \tag{31}$$

where we defined

$$\frac{1}{n_\theta^2} = \frac{\cos^2\theta}{n_o^2} + \frac{\sin^2\theta}{n_e^2} \tag{32}$$

$$n_o^2 = 1 + \chi_o \tag{33}$$

$$n_e^2 = 1 + \chi_e \tag{34}$$

Physically, n_o is the index of refraction for waves polarized in the y-direction and n_θ is the index of refraction for waves polarized in the x-direction. Because n_o is independent of θ, the y-polarized waves are called ordinary waves. Because n_θ has an angular dependence, the x-polarized waves are called extraordinary waves.

F. Nonlinear Polarization Vector

The second order nonlinear polarization vector is related to the electric field through a third rank tensor which is usually given in the crystal basis. By writing out the components of the second order polarization given by

$$\tilde{\mathcal{P}}_i^{(2)} + P_i^{(2)} = \chi_{ijk}\left(E_j + \tilde{\mathcal{E}}_j\right)\left(E_k + \tilde{\mathcal{E}}_k\right) \tag{35}$$

we obtain formulas for $\mathcal{P}^{(2)}$ and $P^{(2)}$ in terms of the usual contracted tensor elements:

$$
\begin{pmatrix} P_x^{(2)} \\ P_y^{(2)} \\ P_z^{(2)} \end{pmatrix} = T \begin{pmatrix} d_{11} & d_{12} & d_{13} & d_{14} & d_{15} & d_{16} \\ d_{21} & d_{22} & d_{23} & d_{24} & d_{25} & d_{26} \\ d_{31} & d_{32} & d_{33} & d_{34} & d_{35} & d_{36} \end{pmatrix} \begin{pmatrix} |\mathcal{E}_u|^2 \\ |\mathcal{E}_v|^2 \\ |\mathcal{E}_w|^2 \\ \mathcal{E}_v^* \mathcal{E}_w + c.c. \\ \mathcal{E}_u^* \mathcal{E}_w + c.c. \\ \mathcal{E}_u^* \mathcal{E}_v + c.c. \end{pmatrix}
\tag{36}
$$

$$
\begin{pmatrix} \mathcal{P}_x^{(2)} \\ \mathcal{P}_y^{(2)} \\ \mathcal{P}_z^{(2)} \end{pmatrix} = 4T \begin{pmatrix} d_{11} & d_{12} & d_{13} & d_{14} & d_{15} & d_{16} \\ d_{21} & d_{22} & d_{23} & d_{24} & d_{25} & d_{26} \\ d_{31} & d_{32} & d_{33} & d_{34} & d_{35} & d_{36} \end{pmatrix} \begin{pmatrix} \mathcal{E}_u E_u \\ \mathcal{E}_v E_v \\ \mathcal{E}_w E_w \\ \mathcal{E}_v E_w + \mathcal{E}_w E_v \\ \mathcal{E}_u E_w + \mathcal{E}_w E_u \\ \mathcal{E}_u E_v + \mathcal{E}_v E_u \end{pmatrix}
\tag{37}
$$

Given a particular propagation geometry the nonlinear susceptibility tensor can be reduced to a scalar denoted by d_{eff}. Unlike the linear susceptibility, d_{eff} is a function of both θ and ϕ even for a uniaxial crystal. The term "uniaxial" is in this sense a misnomer since the crystal is only uniaxial in the linear approximation. Calculation of d_{eff} by hand is time consuming, but by implementing the following procedure using symbolic math software it can be determined easily. Consider first the slowly varying second order polarization vector. Express the six element column vector from Eq. (36) in terms of the laser field components expressed in the laser basis. For example, in place of $\mathcal{E}_u$ put

$$
T^{-1} \begin{pmatrix} \mathcal{E}_x \\ \mathcal{E}_y \\ \mathcal{E}_z \end{pmatrix} \cdot \begin{pmatrix} 1 \\ 0 \\ 0 \end{pmatrix}
\tag{38}
$$

Next, multiply out Eq. (36) given the contracted tensor elements for the crystal of interest (fortunately most of the elements will usually vanish). Also, it is usually a good assumption that the longitudinal field components can be neglected compared to the transverse. Next, determine which polarization components are of interest given the phase matching constraints. For type I phase matching there are two possibilities. In the first case, the THz wave is an ordinary wave and Eq. (36) will reduce to

$$
P_y^{(2)} = d_{\text{eff}}(\theta, \phi) |\mathcal{E}_x|^2
\tag{39}
$$

In the second case the THz wave is an extraordinary wave and Eq. (36) will reduce to

$$P_x^{(2)} = d_{\text{eff}}(\theta, \phi)|\mathcal{E}_y|^2 \tag{40}$$

For type II phase matching, there are two more possibilities. They are as follows:

$$P_x^{(2)} = d_{\text{eff}}(\theta, \phi)(\mathcal{E}_x^*\mathcal{E}_y + c.c.) \tag{41}$$

$$P_y^{(2)} = d_{\text{eff}}(\theta, \phi)(\mathcal{E}_x^*\mathcal{E}_y + c.c.) \tag{42}$$

Note that although we have used the symbol d_{eff} four times, in each case the angular dependence is different. The procedure for computing the value of d_{eff} to use for the rapidly varying polarization is exactly analogous, with the caveat that the factor of 4 from Eq. (37) is *not* absorbed into d_{eff}.

III. DESCRIPTION OF SIMULATION CODE

A. Propagation Equations for the Laser

For the rapidly varying time scale, we account for dispersion by regarding the elements of the susceptibility tensor as operators of the form

$$\hat{\chi}_{ij} = \sum_{k=0}^{\infty} \frac{(-i)^k}{k!} \left.\frac{\partial^k \chi_{ij}}{\partial \omega^k}\right|_{\omega_0} \frac{\partial^k}{\partial t^k} \tag{43}$$

which satisfy the equation

$$\mathcal{P}_i = \hat{\chi}_{ij}\mathcal{E}_j \tag{44}$$

Usually the operators are known in the crystal basis, in which case the laser basis operators can be computed in a way exactly analogous to the dispersionless case:

$$\hat{\chi}_{11} = \hat{\chi}_o \cos^2 \theta + \hat{\chi}_e \sin^2 \theta \tag{45}$$

$$\hat{\chi}_c = (\hat{\chi}_o - \hat{\chi}_e) \cos \theta \sin \theta \tag{46}$$

$$\hat{\chi}_{33} = \hat{\chi}_e \cos^2 \theta + \hat{\chi}_o \sin^2 \theta \tag{47}$$

The wave equation for the complex laser field is obtained by inserting Eq. (8) and the corresponding form for $\mathcal{P}$ into Eq. (25). In the one-dimensional limit this gives

$$\left[(\partial_z - ik_0)^2 - (\partial_t + i\omega_0)^2\right]\mathcal{E}_x = (\partial_t + i\omega_0)^2\mathcal{P}_x \tag{48}$$

$$\left[(\partial_z - ik_0)^2 - (\partial_t + i\omega_0)^2\right]\mathcal{E}_y = (\partial_t + i\omega_0)^2\mathcal{P}_y \tag{49}$$

$$\mathcal{E}_z = -\mathcal{P}_z \tag{50}$$

The polarization components are given by the operator equations

$$\mathcal{P}_x = \hat{\chi}_{11}\mathcal{E}_x + \hat{\chi}_c\mathcal{E}_z + \mathcal{S}_x \tag{51}$$

$$\mathcal{P}_y = \hat{\chi}_o\mathcal{E}_y + \mathcal{S}_y \tag{52}$$

$$\mathcal{P}_z = \hat{\chi}_c\mathcal{E}_x + \hat{\chi}_{33}\mathcal{E}_z + \mathcal{S}_z \tag{53}$$

where $\mathcal{S}_i$ represents all nonlinear contributions to the polarization.

Combining the equations for the x and z components involves an operator inversion. The exact equation for the z-component is

$$(1 + \hat{\chi}_{33})\mathcal{E}_z = -\hat{\chi}_c\mathcal{E}_x - \mathcal{S}_z \tag{54}$$

To invert the operator on the left hand side, first define

$$n_{33}^2 = 1 + \chi_{33}(\omega_0) \tag{55}$$

$$\hat{\delta} = \sum_{k=1}^{\infty} \frac{(-i)^k}{k!} \left.\frac{\partial^k\chi_{33}}{\partial\omega^k}\right|_{\omega_0} \frac{\partial^k}{\partial t^k} \tag{56}$$

so that

$$\left(n_{33}^2 + \hat{\delta}\right)\mathcal{E}_z = -\hat{\chi}_c\mathcal{E}_x - \mathcal{S}_z \tag{57}$$

Far from any resonances, $\hat{\delta} \ll n_{33}^2$. In this case, iteratively multiplying by the conjugate of the operator on the left gives

$$\mathcal{E}_z = -\hat{C}(\hat{\chi}_c\mathcal{E}_x + \mathcal{S}_z) \tag{58}$$

where to second order

$$\hat{C} \approx \frac{1}{n_{33}^2} - \frac{\hat{\delta}}{n_{33}^4} + \frac{\hat{\delta}^2}{n_{33}^6} \tag{59}$$

The propagation equations for the ordinary and extraordinary waves are then

$$\left[(\partial_z - ik_0)^2 - (\partial_t + i\omega_0)^2\right]\mathcal{E}_x = (\partial_t + i\omega_0)^2\left[(\hat{\chi}_{11} - \hat{C}\hat{\chi}_c^2)\mathcal{E}_x - \hat{C}\hat{\chi}_c\mathcal{S}_z + \mathcal{S}_x\right] \tag{60}$$

$$\left[(\partial_z - ik_0)^2 - (\partial_t + i\omega_0)^2\right]\mathcal{E}_y = (\partial_t + i\omega_0)^2(\hat{\chi}_o\mathcal{E}_y + \mathcal{S}_y) \tag{61}$$

B. Propagation Equations for the THz Wave

For the THz field, dispersion is not introduced by regarding the susceptibility as an operator, but rather by coupling the field to a population of harmonic oscillators. The propagation equations can be written down immediately by taking the laser propagation equations, replacing the susceptibility operators with the corresponding constants, taking $\hat{\delta} = 0$, $\omega_0 = 0$, $k_0 = 0$, and by substituting $S_i + H_i$ for $\mathcal{S}_i$. The result is

$$\left(\partial_z^2 - n_\theta^2 \partial_t^2\right) E_x = \partial_t^2 \left[-\frac{\chi_c}{n_{33}^2}(S_z + H_z) + S_x + H_x\right] \tag{62}$$

$$\left(\partial_z^2 - n_o^2 \partial_t^2\right) E_y = \partial_t^2 \left(S_y + H_y\right) \tag{63}$$

where S_i represents all nonlinear contributions to the polarization, and H_i is the polarization due to the harmonic oscillators. The harmonic oscillator polarization is most conveniently computed in the crystal basis where each component satisfies an independent equation of the form

$$\left(\partial_t^2 + \nu_i \partial_t + \Omega_i^2\right) H_i = \rho_i E_i \tag{64}$$

Here the index i refers either to the u, v, or w coordinate, ρ_i is the coupling strength for the given polarization, ν_i is the damping constant for the given polarization, and Ω^2 is the resonant frequency for the given polarization. Once H_i is found in the crystal basis it can easily be expressed in the laser basis using $\mathbf{H}_{LB} = T\mathbf{H}_{CB}$.

Physically, the polarization term H_i represents the coupling of the THz radiation to the vibrations of the crystal lattice. In practical terms, however, what is usually given is the susceptibility and its derivatives with respect to frequency. The parameters ρ_i and Ω_i can be computed from this information by a second order matching of dispersion relations. Suppose the dispersion information for ordinary waves is given by a susceptibility χ and its derivatives. Then the parameters for the propagation equations are

$$\chi_o = 1 + \chi - \left(\frac{\chi''}{\chi'^2} - \frac{1}{\omega_s \chi'}\right)^{-1} \tag{65}$$

$$\Omega_u^2 = \Omega_v^2 = \omega_s^2 + \frac{2\omega_s(\chi - \chi_o)}{\chi'} \tag{66}$$

$$\rho_u = \rho_v = (\chi - \chi_o)(\Omega^2 - \omega_s^2) \tag{67}$$

Here, the prime denotes differentiation with respect to angular frequency with evaluation at ω_s. The parameter ω_s can be any frequency in the THz range where χ and its derivatives are known. The case for χ_e, Ω_w, and ρ_w is exactly analagous.

C.   Numerical Solution of the Propagation Equations

1.   Time Centering and Discrete Grid

Numerical solution of the propagation equations is carried out by differencing the propagation equations on a discrete grid. The "spatial" grid corresponds to the coordinate τ and the "time" levels correspond to the coordinate η. The electric field vectors E_i and $\mathcal{E}_i$ are evaluated at the same spatial grid points (i.e., a staggered spatial grid is not used). At the beginning of a simulation cycle, the laser fields $\mathcal{E}_i$ are known at time levels n and $n+1$. The THz fields E_i are known at time levels $n + 1/2$ and $n + 3/2$. The simulation cycle consists of advancing the laser fields to time level $n + 2$ and the THz fields to time level $n + 5/2$. The laser fields are advanced first. The laser fields from time level n are used to implicitly advance the linear part of the propagation equation. The laser fields from time level $n + 1$ and the THz fields from time levels $n + 1/2$ and $n + 3/2$ are used to include the nonlinear part as an explicitly known, centered, source term. The THz fields are advanced second. The THz fields at $n + 3/2$ and the laser fields at $n + 2$ are used in the explicit advance of the THz fields to time level $n + 5/2$.

2.   Laser Propagation

Expanding the equations for the laser evolution results in a large number of terms. To handle this complexity we utilize symbolic math software to automatically generate the code needed to advance the Eqs. (60) and (61). The procedure utilized by the software program is as follows. First, make the substitutions $\partial_z = \partial_\eta - n_g \partial_\tau$, $\partial_t = \partial_\tau$, and $k_0 = \omega_0 n_o$. Next, expand the equations throwing out all derivatives higher than the first order in η and the second order in τ. Next, substitute difference operators for the differential operators as follows:

$$\partial_\tau \mathcal{E} \rightarrow \frac{[\mathcal{E}(i+1,n) + \mathcal{E}(i+1,n+2)] - [\mathcal{E}(i-1,n) + \mathcal{E}(i-1,n+2)]}{4\Delta\tau} \tag{68}$$

$$\partial_\tau^2 \mathcal{E} \rightarrow \frac{[\mathcal{E}(i+1,n) + \mathcal{E}(i+1,n+2)] - 2[\mathcal{E}(i,n) + \mathcal{E}(i,n+2)] + [\mathcal{E}(i-1,n) + \mathcal{E}(i-1,n+2)]}{2\Delta\tau^2}$$

$$\tag{69}$$

$$\partial_{\eta\tau} \mathcal{E} \rightarrow \frac{[\mathcal{E}(i+1,n+2) - \mathcal{E}(i-1,n+2)] - [\mathcal{E}(i+1,n) - \mathcal{E}(i-1,n)]}{4\Delta\eta\Delta\tau} \tag{70}$$

$$\partial_\eta \mathcal{E} \rightarrow \frac{\mathcal{E}(i, n+2) - \mathcal{E}(i, n)}{2\Delta\eta} \tag{71}$$

Here $\mathcal{E}$ is either electric field component, i is the grid cell, n is the "time" level, $\Delta\tau$ is the cell size and $\Delta\eta$ is the timestep. The resulting equation will always take the form

$$T_1\mathcal{E}(i-1, n+2) + T_2\mathcal{E}(i, n+2) + T_3\mathcal{E}(i+1, n+2) = K_1\mathcal{E}(i-1, n) + K_2\mathcal{E}(i, n) + K_3\mathcal{E}(i+1, n) + C \tag{72}$$

Note that the nonlinear terms are contained in C and are centered since they are known at time level $n + 1$. The final outputs from the symbolic math software are expressions for T_i, K_i, and C. To eliminate transcription error, it is best to have the software generate the expressions in a format compatible with the programming language being used for the simulation so that the expressions can be pasted directly into the code. Once these expressions are in the code a standard tridiagonal algorithm can be used to advance $\mathcal{E}_i$.

3. THz Propagation

Rewriting the THz propagation equations in terms of the laser frame coordinates and taking $\partial_\eta^2 \rightarrow 0$ gives

$$(v_\theta\partial_\eta + \partial_\tau) E_x = \frac{\partial_\tau}{n_g^2 - n_\theta^2} \left[-\frac{\chi_c}{n_{33}^2}(S_z + H_z) + S_x + H_x \right] \tag{73}$$

$$(v_o\partial_\eta + \partial_\tau) E_y = \frac{\partial_\tau}{n_g^2 - n_o^2} [S_y + H_y] \tag{74}$$

where

$$v_\theta = \frac{2n_g}{n_\theta^2 - n_g^2} \tag{75}$$

$$v_o = \frac{2n_g}{n_o^2 - n_g^2} \tag{76}$$

The equation for the lattice vibration in the laser frame is

$$\left(\partial_\tau^2 + \nu_i\partial_\tau + \Omega_i^2 \right) H_i = \rho_i E_i \tag{77}$$

The nonlinear polarization S_i is computed from the laser field using Eq. (36).

The problem is to advance E_i from timestep $n + 3/2$ to timestep $n + 5/2$ given that we know H_i at timestep $n + 3/2$ and S_i at timestep $n + 2$. Since H_i is effectively a function of

E_i, the equations for E_i can be put in the form of the flux conservative initial value problem $\partial_\eta E_i = -\partial_\tau F_i(E_i)$ where

$$F_x = \frac{E_x}{v_\theta} - \frac{S_x + H_x - \chi_c(S_z + H_z)/n_{33}^2}{v_\theta(n_g^2 - n_\theta^2)} \tag{78}$$

$$F_y = \frac{E_y}{v_o} - \frac{S_y + H_y}{v_o(n_g^2 - n_o^2)} \tag{79}$$

These can be solved using the standard Lax-Wendroff method where H_i is regarded as a function of E_i and S_i is regarded as constant.

4. Longitudinal Fields

Although the longitudinal fields do not appear explicitly in the propagation equations, they are needed to compute the nonlinear source terms and the lattice vibrations. In the laser advance, the nonlinear source terms $\mathcal{S}_i$ are needed at time level $n + 1$, and therefore *all* the components $\mathcal{E}_i$ and E_i are also needed at time level $n + 1$. These will be available provided all the components including $\mathcal{E}_z$ were advanced to time level $n + 2$ on the previous cycle. To accomplish this, we first advance $\mathcal{E}_x$ as described above, and then use the linearized Eq. (58) to estimate $\mathcal{E}_z$:

$$\mathcal{E}_z \approx -\hat{C}\hat{\chi}_c\mathcal{E}_x \tag{80}$$

In the THz advance, the lattice vibrations H_i depend on the longitudinal field E_z. Therefore, at the midpoint of the Lax-Wendroff calculation we estimate E_z based on the slowly varying analog of Eq. (58):

$$E_z = -\frac{\chi_c E_x + H_z + S_z}{1 + \chi_{33}} \tag{81}$$

We then recalculate H_i based on this new field. At the end of the Lax-Wendroff calculation, we repeat this procedure twice in order to iteratively improve the accuracy of both E_z and H_i for use during the next cycle.

5. Magnetic Field and Energy Diagnostic

Although the magnetic field is not needed to advance the propagation equations, it is useful for diagnostic purposes. In particular, it can be used in the calculation of the energy

contained in the laser oscillations and the THz oscillations so that the conversion efficiency can be calculated, and energy conservation can be verified.

For the magnetic field associated with the laser energy, we first compute the linear part of the polarization using Eq. (44) and then use

$$\mathcal{B}_x = -\frac{\mathcal{E}_y + \mathcal{P}_y}{n_g} \tag{82}$$

$$\mathcal{B}_y = \frac{\mathcal{E}_x + \mathcal{P}_x}{n_g} \tag{83}$$

$$\mathcal{B}_z = 0 \tag{84}$$

which is an approximation based on Ampere's law. Note that dispersion can affect the proportion of energy carried by the magnetic field. Remembering the summation convention, the energy density carried by the fast laser oscillations is

$$u_f = \frac{\mathcal{E}_i \mathcal{E}_i^* + \mathcal{B}_i \mathcal{B}_i^*}{4} + \frac{\mathcal{E}_i^* \mathcal{P}_i + \mathcal{E}_i \mathcal{P}_i^*}{8} \tag{85}$$

For the magnetic field associated with the THz energy, the linear part of the polarization can be found from

$$P_x = \left(n_\theta^2 - 1\right) E_x + H_x \tag{86}$$

$$P_y = \left(n_o^2 - 1\right) E_y + H_y \tag{87}$$

$$P_z = -E_z \tag{88}$$

The THz magnetic field can then be computed from expressions exactly analogous to those for the laser field. The energy density can then be computed using

$$u_s = \frac{E_i E_i + B_i B_i + E_i P_i}{2} \tag{89}$$

IV.   ANALYSIS OF OPTICAL RECTIFICATION

A.   Driving Terms for Gallium Selenide

To date, the conversion of optical to THz power has been most efficient when Gallium Selenide (GaSe) was used as the nonlinear material [9]. We therefore use GaSe as an example in all that follows. The symmetries of the GaSe lattice require that all components of the nonlinear susceptibility vanish except for d_{16}, d_{21}, and d_{22}. Furthermore, $d_{16} = d_{21} = -d_{22} \approx$

50×10^{-12} m/V. Using the technique outlined in section II F, the transverse components of the slowly varying nonlinear polarization vector can be determined to have the following dependence on the applied laser field and the crystal orientation:

$$P_x^{(2)} = d_{16} \cos\theta \left[-\cos^2\theta \sin 3\phi |\mathcal{E}_x|^2 + \sin 3\phi |\mathcal{E}_y|^2 + \cos\theta \cos 3\phi (\mathcal{E}_x \mathcal{E}_y^* + \mathcal{E}_x^* \mathcal{E}_y) \right] \tag{90}$$

$$P_y^{(2)} = d_{16} \left[\cos^2\theta \cos 3\phi |\mathcal{E}_x|^2 - \cos 3\phi |\mathcal{E}_y|^2 + \cos\theta \sin 3\phi (\mathcal{E}_x \mathcal{E}_y^* + \mathcal{E}_x^* \mathcal{E}_y) \right] \tag{91}$$

Typically, because of phase matching considerations, only one of the six driving terms from the above two equations will be important. Furthermore, it is virtually always the case that in order for phase matching to be achieved, the driving term must contain the polarization component orthogonal to the driven term. Hence, the expressions for the polarization components can usually be reduced to one of the following:

$$P_x^{(2),\mathrm{I}} = d_{16} \cos\theta \sin 3\phi |\mathcal{E}_y|^2 \tag{92}$$

$$P_y^{(2),\mathrm{I}} = d_{16} \cos^2\theta \cos 3\phi |\mathcal{E}_x|^2 \tag{93}$$

$$P_x^{(2),\mathrm{II}} = d_{16} \cos^2\theta \cos 3\phi (\mathcal{E}_x \mathcal{E}_y^* + \mathcal{E}_x^* \mathcal{E}_y) \tag{94}$$

$$P_y^{(2),\mathrm{II}} = d_{16} \cos\theta \sin 3\phi (\mathcal{E}_x \mathcal{E}_y^* + \mathcal{E}_x^* \mathcal{E}_y) \tag{95}$$

Here, the superscripts I and II refer to type I and type II phase matching, respectively. The definition of type I phase matching is that the driving term contains only one polarization component. The definition of type II phase matching is that the driving term contains both polarization components.

In the case of the nonlinear polarization at the laser frequency, the expressions for the transverse components are

$$\mathcal{P}_x^{(2)} = 4d_{16} \left[\cos^2\theta \cos 3\phi \left(\mathcal{E}_x E_y + \mathcal{E}_y E_x \right) - \cos\theta \sin 3\phi \left(\mathcal{E}_x E_x \cos^2\theta - \mathcal{E}_y E_y \right) \right] \tag{96}$$

$$\mathcal{P}_y^{(2)} = 4d_{16} \left[\cos 3\phi \left(\mathcal{E}_x E_x \cos^2\theta - \mathcal{E}_y E_y \right) + \cos\theta \sin 3\phi \left(\mathcal{E}_x E_y + \mathcal{E}_y E_x \right) \right] \tag{97}$$

For type I phase matching, these can be reduced to one of the following:

$$\mathcal{P}_x^{(2),I} = 4d_{16} \cos^2\theta \cos 3\phi \mathcal{E}_x E_y \tag{98}$$

$$\mathcal{P}_y^{(2),I} = 4d_{16} \cos\theta \sin 3\phi \mathcal{E}_y E_x \tag{99}$$

B. Phase Matching Condition and THz Evolution

An expression for the signal produced by optical rectification in the presence of an arbitrary phase mismatch can be found if pump depletion and dispersion are neglected. In the case of a type I interaction, dropping the dispersive terms from Eq. (73), and assuming $S_z \ll S_x$, gives

$$\left(v_\theta \partial_\eta + \partial_\tau\right) E_x = \frac{d_{\text{eff}}}{n_g^2 - n_\theta^2} \partial_\tau |\mathcal{E}_y|^2 \tag{100}$$

where for a GaSe crystal

$$d_{\text{eff}} = d_{16} \cos\theta \sin 3\phi \tag{101}$$

Making a second coordinate transformation $Z = \eta$ and $T = \tau - \eta/v_\theta$ gives

$$\partial_Z E_x = -\frac{d_{\text{eff}}}{2n_g} \partial_T |\mathcal{E}_y|^2 \tag{102}$$

The integral representation of E_x is

$$E_x = -\frac{d_{\text{eff}}}{2n_g} \int_0^Z \partial_T |\mathcal{E}_y|^2 dZ' \tag{103}$$

The integral cannot be solved in this form because $\mathcal{E}_y$ is a function of both T and Z. However, if pump depletion and dispersion are neglected, $\mathcal{E}_y$ is independent of η. We therefore rewrite the integral as

$$E_x = -\frac{d_{\text{eff}}}{2n_g} \int_T^\tau \partial_{\tau'} |\mathcal{E}_y(\tau')|^2 v_\theta d\tau' \tag{104}$$

which can be solved immediately. Defining $\epsilon = \eta/v_\theta$ we obtain

$$E_x = -\frac{d_{\text{eff}}}{2n_g} \frac{\eta}{\epsilon} \left(|\mathcal{E}_y(\tau)|^2 - |\mathcal{E}_y(\tau - \epsilon)|^2 \right) \tag{105}$$

For finite ϵ, as the propagation distance η increases the two terms in Eq. (105) become well separated in time and the peak signal amplitude converges to the finite value

$$E_{\text{peak}} = \frac{d_{\text{eff}} |\mathcal{E}_0|^2}{|n_\theta^2 - n_g^2|}, \qquad \eta \gg v_\theta \tau_L \tag{106}$$

where $\mathcal{E}_0$ is the peak electric field of the laser pulse and τ_L is the laser pulse length. Convergence of the signal to a finite value is not characteristic of a phase matched interaction. The case where $\epsilon = 0$ can be analyzed by expanding Eq. (105) in powers of ϵ:

$$E_x = -\frac{d_{\text{eff}}}{2n_g} \eta \left(\partial_\tau + \frac{\epsilon \partial_\tau^2}{2!} + \frac{\epsilon^2 \partial_\tau^3}{3!} + \ldots \right) |\mathcal{E}_y(\tau)|^2 \tag{107}$$
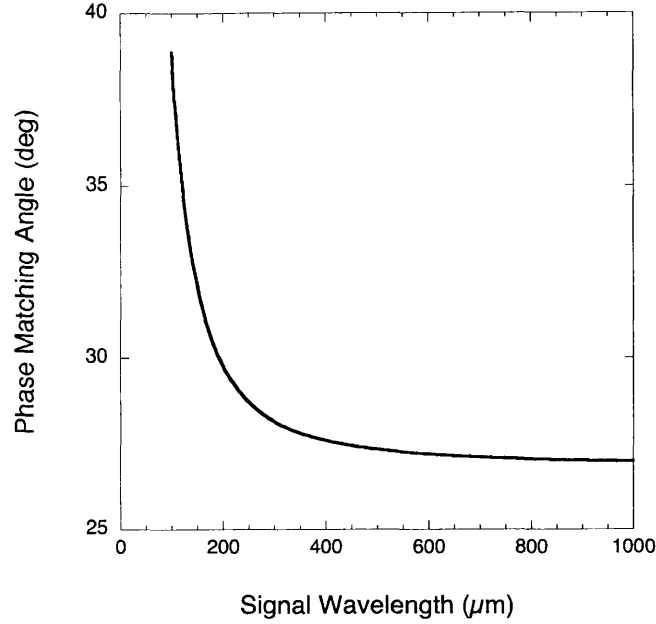
FIG. 1: Angle tuning curve for optical rectification in GaSe using 800 nm radiation as the pump.

Substituting $\epsilon = 0$ then gives a signal amplitude that grows indefinitely with η. The phase matching condition is therefore $\epsilon = 0$. The waveform of the signal in this case is just the derivative of the laser envelope. For a typical laser pulse shape, the signal will be a single cycle pulse with center frequency $\omega_s = \pi/\tau_L$.

A more physically revealing form of the phase matching condition is

$$n_\theta(\omega_s) = n_g(\omega_0) \tag{108}$$

In other words, the phase velocity of the THz radiation must equal the group velocity of the laser pulse. This condition arises because the phase of the source (i.e., the nonlinear polarization wave) at a given point is determined by the derivative of the envelope of the laser pulse at that point. Therefore the phase of the source stays synchronous with the phase of the THz wave when the laser envelope moves at the THz phase velocity. Fig. 1 shows the phase matching angle in GaSe as a function of signal wavelength for an 800 nm pump laser. The curve was calculated by solving $n_\theta(\omega_s) = n_g(\omega_0)$ using the GaSe dispersion relation from Ref. [12].

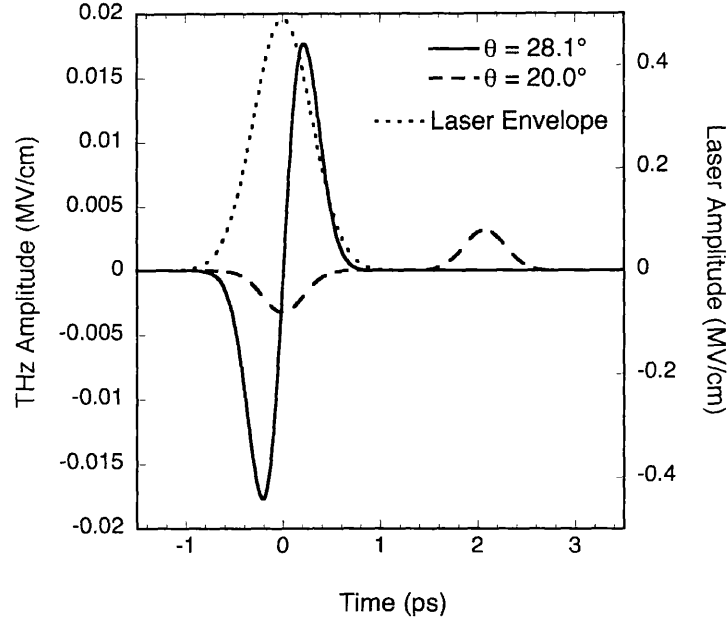For a perfectly phase matched interaction, the signal amplitude can always be increased

FIG. 2: Time dependence of the THz electric field after 1 cm of propagation for two matching conditions. The solid line is the THz field for a negligible phase mismatch of 0.01%. The dashed line is the THz field for a mismatch of 2.0%. The dotted line shows the magnitude of the complex envelope of the laser field.

by increasing the interaction length, η. In the case of a significant phase mismatch, Eq. (106) suggests that E_{peak} could still become large if either $|\mathcal{E}_0|^2$ or d_{eff} are large. Unfortunately, as discussed in section IV D, $|\mathcal{E}_0|^2$ is limited by the two-photon absorption process. On the other hand, media with very large values of d_{eff}, such as electric field biased AlGaAs quantum wells and GaAs/AlGaAs asymmetric quantum wells [13, 14], might make it possible to generate large amplitude THz waves without the need for phase matching.

As an example of a phase matched interaction, consider the generation of 1.0 THz radiation in GaSe using a pump intensity of 1 GW/cm^2. The signal frequency fixes the laser pulse length to $\tau_L = 500$ fs. Figure 2 shows the time dependence of the THz electric field as computed from Eq. (105) evaluated after 1 cm of propagation for two matching conditions. The solid line corresponds to $\theta = 28.1°$ which gives $|n_g(\omega_0) - n_\theta(\omega_s)|/n_g(\omega_0) = 0.01\%$. The dashed line corresponds to $\theta = 20.0°$ which gives $|n_g(\omega_0) - n_\theta(\omega_s)|/n_g(\omega_0) = 2.0\%$. The
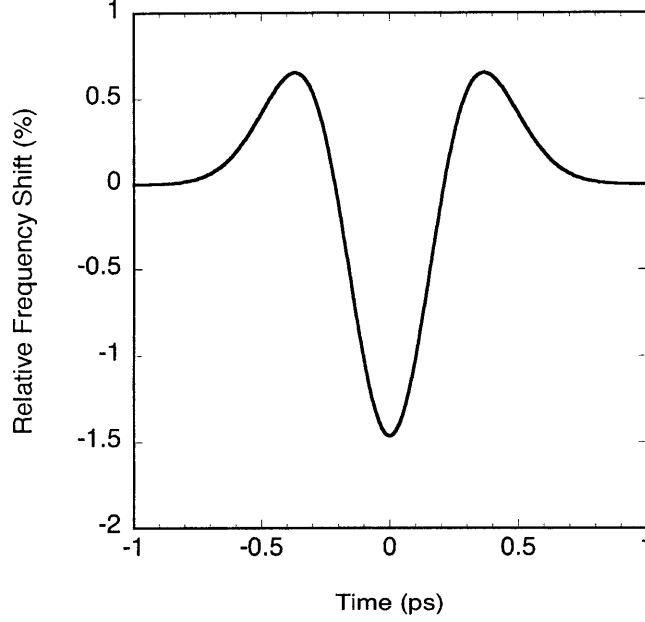
FIG. 3: Instantaneous frequency shift $\Delta\omega/\omega_0$ of the pump after 1 cm of propagation in GaSe in the case where dispersion is neglected. The intensity of the pump is 1 GW/cm^2.

dotted line shows the laser envelope on a different scale. As expected from the expansion solution, the matched case is approximately the time derivative of the Laser envelope. In the mismatched case, the time separation between the positive and negative polarity portions of the pulse increases with propagation distance, but the signal amplitude remains constant.

C. Pump Depletion and Pulse Compression

The effect of the signal field on the laser is to deplete the laser energy and compress the laser pulse. Assuming perfect type I phase matching ($n_o = n_\theta = n_g$) and neglecting dispersion allows the propagation equation for the laser to be reduced to

$$\left(\partial_\eta^2 - 2n_g\partial_{\eta\tau} - 2i\omega_0 n_g\partial_\eta\right)\mathcal{E}_y = (\partial_\tau + i\omega_0)^2\mathcal{S}_y \tag{109}$$

Assuming $\partial_\tau \ll \omega_0$, $\chi_c\mathcal{S}_z/n_{33}^2 \ll \mathcal{S}_x$, and $\partial_\eta^2 \to 0$, this can be further simplified to

$$\partial_\eta\mathcal{E}_y = -\frac{2i\omega_0}{n_g}d_{\text{eff}}\mathcal{E}_y E_x \tag{110}$$

A first order perturbation analysis of this equation gives

$$\mathcal{E}_y = \mathcal{E}_0 - \frac{2i\omega_0}{n_g}\eta d_{\text{eff}}\mathcal{E}_0 E_x \tag{111}$$

where $\mathcal{E}_0$ is the initial laser field. Inserting Eq. (107) for E_x and taking $\epsilon = 0$ gives

$$\mathcal{E}_y = \mathcal{E}_0\left(1 + \frac{i\omega_0}{n_g^2}d_{\text{eff}}^2\eta^2\partial_\tau|\mathcal{E}_0|^2\right) \tag{112}$$

The argument of the factor in parenthesis gives the instantaneous phase shift. Taking the time derivative of this phase gives the instantaneous frequency shift

$$\frac{\Delta\omega}{\omega_0} = \eta^2\frac{d_{\text{eff}}^2}{n_g^2}\partial_\tau^2|\mathcal{E}_0|^2 \tag{113}$$

The instantaneous frequency shift is plotted in Fig. 3 for the same parameters that were used in Fig. 2. The frequency shift is proportional to the second derivative of the laser envelope.

It is instructive to consider the frequency shift just derived in terms of an analogy with self phase modulation. In self phase modulation, the nonlinear polarization is $P^{(3)} = C|\mathcal{E}|^2\mathcal{E}$, where $\mathcal{E}$ is any component of the laser field and C is a factor independent of $\mathcal{E}$. This leads to an intensity dependent refractive index $n_3 = n_1 + C|\mathcal{E}|^2/2n_1$, where n_1 is the linear part of the refractive index. This leads to a frequency shift proportional to $\partial_\tau|\mathcal{E}|^2$. In the present case, the nonlinear polarization is $P^{(2)} = 4d_{\text{eff}}E\mathcal{E} = K(\partial_\tau|\mathcal{E}|^2)\mathcal{E}$, where K is a factor independent of $\mathcal{E}$. The intensity dependent refractive index in this case is $n_2 = n_1 + K(\partial_\tau|\mathcal{E}|^2)/2n_1$. Comparing n_2 and n_3 makes it obvious that if n_3 leads to a frequency shift proportional to $\partial_\tau|\mathcal{E}|^2$, then n_2 leads to a frequency shift proportional to $\partial_\tau^2|\mathcal{E}|^2$.

A photon kinetic picture [15, 16] can be used to show that in the presence of group velocity dispersion, the frequency shift induced by the THz field causes a portion of the laser pulse to compress. Let $\tau' = t - n_g z'$ where z' is the coordinate of a photon in the Lagrangian (as opposed to Eulerian) picture. The motion of the photon is then described by

$$\frac{d\tau'}{d\eta} = \beta_2\Delta\omega \tag{114}$$

where $\hbar(\omega_0 + \Delta\omega)$ is the energy of the photon and β_2 is the usual group velocity dispersion coefficient defined as the second order term in the sequence

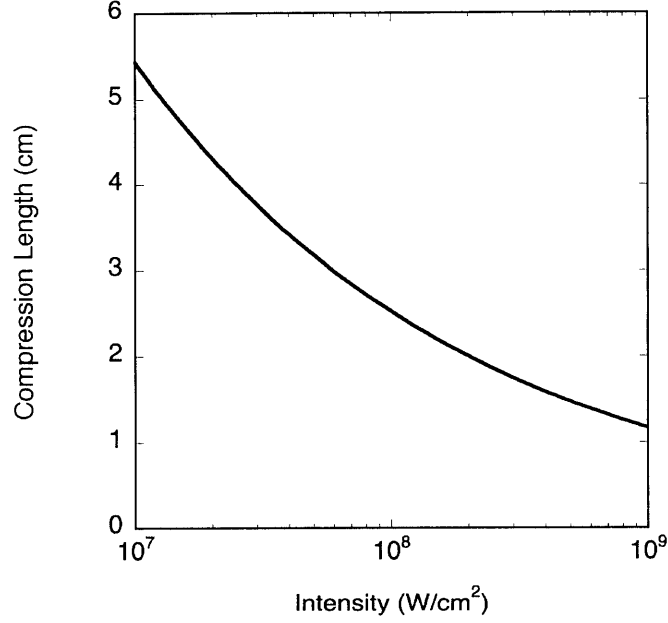$$\beta_i = \frac{\partial^i}{\partial\omega^i}(n_o\omega) \tag{115}$$

FIG. 4: Length of GaSe crystal needed to maximally compress an 800 nm wavelength pump pulse.

After the pulse propagates a distance L, a photon initially at $\tau' = 0$ moves to

$$\tau' = \int_0^L \beta_2 \Delta\omega \, d\eta \qquad (116)$$

We approximate $\Delta\omega$ by evaluating Eq. (113) at $\tau = 0$ and using for the initial pulse shape

$$\mathcal{E}_0 = \mathcal{E}_{00} \exp\left(-2\ln 2\frac{\tau^2}{\tau_L^2}\right) \qquad (117)$$

This procedure assumes that $\tau' \ll \tau_L$. In this case, the photon position is

$$\tau' = -\frac{8\ln 2}{3}\frac{\beta_2\omega_0}{\beta_1^2}\frac{d_{\text{eff}}^2\mathcal{E}_{00}^2}{\tau_L^2}L^3 \qquad (118)$$

The sign of β_2 is usually positive, which means that the downshifted photons at the center of the pulse will tend to drift toward the upshifted photons at the front of the pulse. An estimate of the point of maximum compression can be obtained by setting $\tau' = -\tau_L/2$ and solving for L. This gives

$$L_{\text{comp}} = \tau_L \left(\frac{3}{16\ln 2}\frac{\beta_1^2}{\beta_2\omega_0}\frac{1}{d_{\text{eff}}^2\mathcal{E}_{00}^2}\right)^{1/3} \qquad (119)$$

The compression length as a function of pump intensity is shown in Fig. 4 for the same parameters that were used in Fig. 2. For a GaSe crystal, $\beta_2 \approx 4 \times 10^{-16}$ seconds for 800 nm radiation.

D. Two Photon Ionization

The highest intensity useful for optical rectification is reached when the electron hole plasma becomes dense enough to reflect THz radiation. It can be shown that the absorption of radiation due to ionization processes and carrier scattering is described by

$$\frac{\partial I}{\partial \eta} = -U_i \frac{\partial n_e}{\partial \tau} - n_e \sigma_h I \tag{120}$$

where U_i is the energy required to bring an electron from the valence to the conduction band, n_e is the free electron density, and σ_h is the cross section for hole scattering. Hole scattering leads to collisional losses through inverse bremstrahlung. For GaSe, the bandgap energy is $E_g = 2.0$ eV, and $\sigma_h \approx 5 \times 10^{-17}$ cm^2 [17]. For 800 nm light, the photon energy is about 1.55 eV, so ionization occurs via a two photon mechanism, and $U_i = 3.1$ eV. In this case, the free electron density evolves according to

$$\frac{\partial n_e}{\partial \tau} = \frac{\beta}{U_i} I^2 \tag{121}$$

where β is the usual two-photon absorption coefficient. For GaSe, $\beta \approx 0.558$ cm/GW for 800 nm radiation and a 1 ps pulse length [18]. The maximum intensity useful for the generation of THz radiation is the intensity for which the free electron density reaches the critical density

$$n_{\text{crit}} = \omega^2 \left(\frac{1}{m_e^*} + \frac{\alpha}{m_h^*} + \frac{1-\alpha}{m_l^*} \right)^{-1} \tag{122}$$

where ω is the frequency of the THz radiation, m_e^* is the effective mass of an electron, m_h^* is the effective mass of heavy holes, m_l^* is the effective mass of light holes, and α is the fraction of holes that are heavy holes. For GaSe, $m_e^* \approx 0.2$. To obtain an estimate of the maximum useful intensity, we combine Eqs. (121) and (122), take the laser pulse length to be 500 fs, assume $\alpha \approx 1$ and $m_h^* \gg m_e^*$:

$$I_{\text{max}} = \left(\frac{\omega^2 m_e^* U_i}{\beta \tau_L} \right)^{1/2} = 2.1 \text{ GW/cm}^2 \tag{123}$$

TABLE II: Simulation Parameters

Quantity	Value
Crystal	GaSe
Dispersion Parameters	See Ref. [12]
Lattice damping constant	$\nu = 125$ GHz
Two photon ionization coefficient	$\beta = 0$
Laser Intensity	1 GW/cm^2
Laser Wavelength	$\lambda_0 = 800$ nm
Laser Pulselength	$\tau_L = 500$ fsec
Signal Frequency	1.0 THz
Phase Matching Configuration	Type I
Phase Matching Angle	$\theta = 28.1°$
Azimuthal rotation	$\phi = 30°$
Laser Polarization	ordinary
THz Polarization	extraordinary

It should be noted that at this intensity the electron-hole plasma will significantly modify the dispersion relation for the THz radiation which will in turn modify the phase matching condition. In addition, the value of I_{max} given in Eq. (123) will be substantially reduced if the value of β measured in earlier experiments [19, 20] is used.

V. SIMULATIONS

The simulation model described in section III extends the regime of validity of the analysis in that it self-consistently includes dispersion of both the THz and laser pulses, pump depletion, and THz losses due to vibrational damping. In this section, we compare the analysis with simulation results obtained using different sets of approximations. The parameters used are given in Table II.

First, the analytical result shown in Fig. 2 is reproduced by running the simulation with dispersion neglected. The simulation results are shown in Fig. 5. The two results are almost
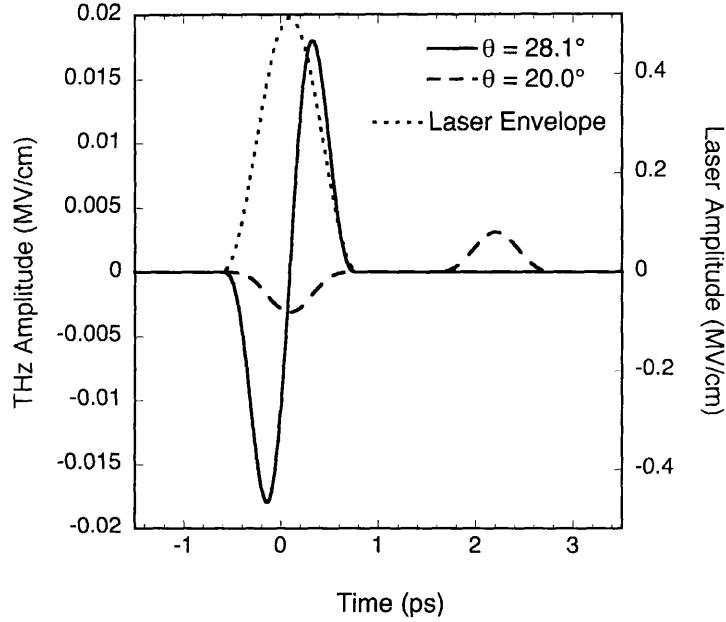
FIG. 5: Simulation with dispersion turned off showing agreement with the analytically predicted THz waveforms in the case of a phase-matched and non-phase-matched interaction (cf. Fig. 2).

indistinguishable. Note that pump depletion was not neglected, but its effect was minimal due to the low conversion efficiency over 1 cm of propagation.

From the same simulation, a comparison can be made with the analytical prediction for the frequency shift from Fig. 3. The corresponding simulation result is shown in Fig. 6. The simulation data is displayed as a Wigner transform of the laser electric field. The Wigner transform is characterized by the following properties: (i) when integrated over time it gives the frequency spectrum of the pulse (ii) when integrated over frequency it gives the time domain representation of the pulse (iii) it becomes a photon distribution function in the limit of geometric optics. The frequency shift indicated by the Wigner transform is similar to the instantaneous frequency shift from Fig. 3.

As an additional check, Fig. 7 shows the energy gained by the THz radiation and the energy lost by the laser pulse for the same simulation used to generate Figs. 5 and 6. The simulation conserves energy to a high degree of accuracy.

Next, the simulation is repeated with dispersion included, and the propagation distance
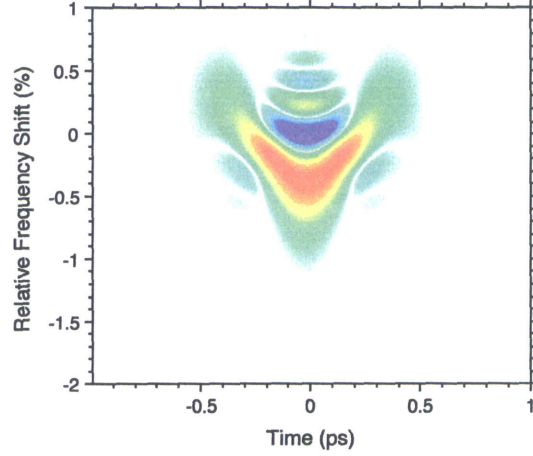
FIG. 6: Wigner transform of the laser electric field after 1 cm of propagation in the absence of dispersion.
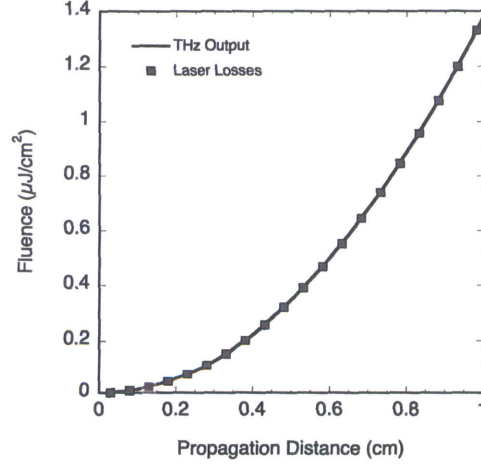

FIG. 7: Energy conservation in the case of zero dispersion.

is extended far enough to observe saturation of the conversion efficiency. The damping constant associated with the lattice vibrations is set to $\nu = 125$ GHz in order to give an absorption coefficient consistent with Ref. [6]. The conversion efficiency as a function of propagation distance is shown in Fig. 8. A conversion efficiency of 1.5% is obtained before saturation occurs at about $z = 5$ cm. Note that the Manley-Rowe limit is exceeded by about a factor of 5. The THz waveform at $z = 5$ cm is shown in Fig. 9. The waveform departs
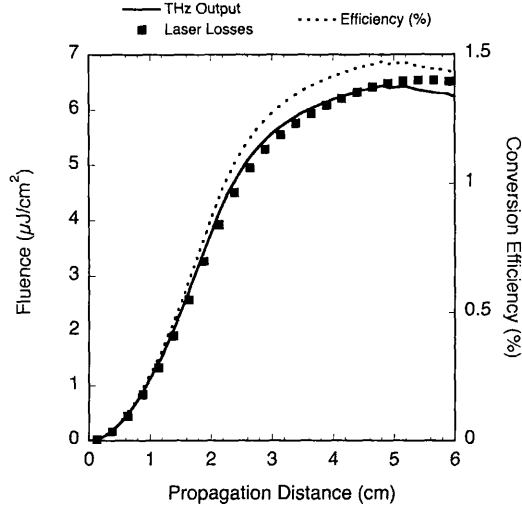
FIG. 8: Energy conservation with dispersion and vibrational damping.

from the single cycle pulse characteristic of optical rectification because of the dispersive terms H_i.

Finally, Fig. 10 shows the laser pulse shape at four propagation distances. As localized frequency shifts develop, pulse compression occurs at the head of the pulse due to group velocity dispersion. In this case, the point of maximum compression occurs at about $z = 2.1$ cm, which is about twice the analytical prediction from Fig. 4. The fact that the group velocity and pulse shape both change during the course of the interaction causes the phase mismatch to increase with increasing z. This eventually leads to saturation of the conversion efficiency. It should be noted that in this example the two-photon ionization rate increases by about a factor of 12 as the laser propagates from $z = 0$ cm to $z = 2$ cm. At the same time, the pulse length is is reduced by a factor of 5. The electron hole plasma, therefore, is about twice as dense at $z = 2$ cm than at $z = 0$ cm. This could strongly affect the results, and will be the subject of future study.

VI. SUMMARY

Optical rectification of short laser pulses in nonlinear crystals can generate high peak power THz radiation. The GaSe crystal appears to be promising for this application due to its high nonlinearity, low losses, and favorable phase matching characteristics. Analysis and
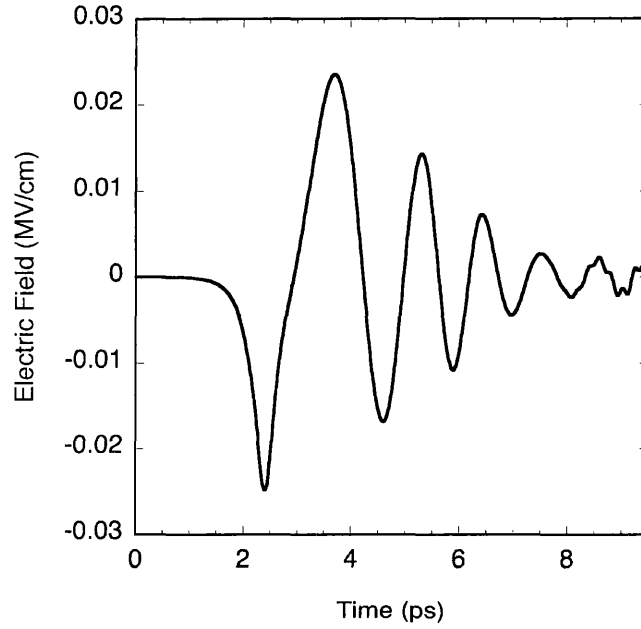
FIG. 9: Time domain waveform of the THz signal after 5 cm of propagation

simulations both indicate that an 800 nm laser pulse with a pulse width of 500 fs can be phase matched in GaSe to produce 1.0 THz radiation with a peak power of about 1 MW. The conversion efficiency saturates at about 1 percent due to frequency shifts in the laser pulse which cause it to compress and accelerate. Also, it should be noted that the configuration considered here requires that index matching materials be used to couple radiation into and out of the GaSe crystal. In the future, the electron-hole plasma will be incorporated directly into the simulation model so that its effects on the conversion efficiency can be more accurately determined.
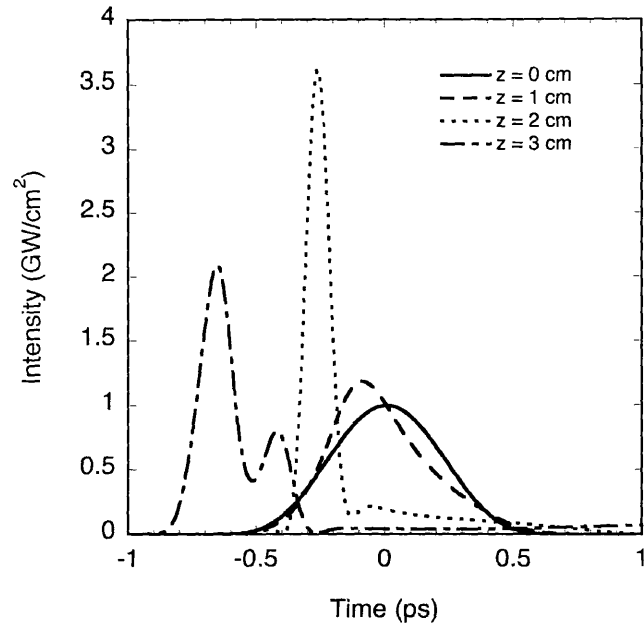
FIG. 10: Temporal shape of the laser pulse evaluated at four propagation distances. Note that the increasing laser intensity will increase the two-photon ionization rate.

VII. ACKNOWLEDGEMENTS

[1] D. Strickland and G. Mourou. Compression of amplified chirped optical pulses. *Opt. Comm.*, 56(3):219–221, 1985.

[2] D.H. Auston. Subpicosecond electro-optic shock waves. *Appl. Phys. Lett.*, 43(8):713–715, October 1983.

[3] Z. Jiang and X.-C. Zhang. Free-space electro-optic techniques. In *Sensing with terahertz radiation*. Springer.

[4] R. Huber, A. Brodschelm, F. Tauser, and A. Leitenstorfer. Generation and field-resolved detection of femtosecond electromagnetic pulses tunable up to 41 Thz. *Appl. Phys. Lett.*,

76(22):3191–3193, May 2000.

[5] Y.-S. Lee, T. Meade, V. Perlin, H. Winful, and T.B. Norris. Generation of narrow-band terahertz radiation via optical rectification of femtosecond pulses in periodically poled lithium niobate. *Appl. Phys. Lett.*, 76(18):2505–2507, May 2000.

[6] Y.J. Ding and I.B. Zotova. Second-order nonlinear optical materials for efficient generation and amplification of temporally-coherent and narrow-linewidth terahertz waves. *Optical and Quantum Electronics*, 32:531–552, 2000.

[7] Y.S. Lee, T. Meade, and T.B. Norris. Tunable narrow-band terahertz generation from periodically poled lithium niobate. *Appl. Phys. Lett.*, 78(23):3583–3585, June 2001.

[8] J.Z. Xu and X.-C. Zhang. Optical rectification in an area with a diameter comparable to or smaller than the center wavelength of terahertz radiation. *Opt. Lett.*, 27(12):1067–1069, June 2002.

[9] W. Shi, Y.J. Ding, N. Fernelius, and K. Vodopyanov. Efficient, tunable, and coherent 0.18-5.27-thz source based on GaSe crystal. *Optics Lett.*, 27(16):1454–1456, Aug 2002.

[10] Wei Shi and Yujie Ding. Continuously tunable and coherent terahertz radiation by means of phase-matched difference-frequency generation in zinc germanium phosphide. *Appl. Phys. Lett.*, 83(5):848–850, August 2003.

[11] W. Shi and Y.J. Ding. A monochromatic and high-power terahertz source tunable in the ranges of 2.7-38.4 and 58.2-3540 μm for variety of potential applications. *Appl. Phys. Lett.*, 84(10):1635–1637, March 2004.

[12] V.G. Dimitriev, G.G. Gurzadyan, and D.N. Nikogosyan. *Handbook of Nonlinear Optical Crystals*. Springer, Heidelberg, 1999.

[13] M.M. Fejer, S.J.B. Yoo, R.L. Beyer, A. Harwit, and J.S. Harris. Observation of extremely large quadratic susceptibility at 9.6-10.8 μm in electric field biased AlGaAs quantum wells. *Phys. Rev. Lett.*, 62:1041, 1989.

[14] P. Boucaud, F.H. Julien, D.D. Yang, J-M. Lourtioz, E. Rosencher, P. Bois, and J. Nagle. Detailed analysis of second harmonic generation near 10.6 μm in GaAs/AlGaAs asymmetric quantum wells. *Appl. Phys. Lett.*, 57(3):215–217, July 1990.

[15] I.M. Besieris and F.D. Tappert. Stochastic wave-kinetic theory in the Liouville approximation. *J. Mathematical Phys.*, 17(5):734–743, May 1976.

[16] L. Silva and J.T. Mendonca. Kinetic theory of photon acceleration: time dependent spectral

evolution of ultrashort laser pulses. *Phys. Rev. E*, 57(3):3423–3431, Mar 1998.

[17] J. H. Bechtel and W. L. Smith. Two-photon absorption in semiconductors with picosecond laser pulses. *Phys. Rev. B*, 13(8):3515–3522, Apr 1976.

[18] I. B. Zotova and Y. J. Ding. Spectral measurements of two-photon absorption coefficients for CdSe and GaSe crystals. *Appl. Optics*, 40(36):6654–6658, Dec 2001.

[19] F. Adduci, I.M. Catalano, A. Cingolani, and A. Minafra. Direct and indirect two-photon processes in layered semiconductors. *Phys. Rev. B*, 15(2):926–931, January 1977.

[20] K.L. Vodopyanov, S.B. Mirov, V.G. Voevodin, and P.G. Schunemann. Two-photon absorption in GaSe and $CdGeAs_2$. *Opt. Comm.*, 155:47–50, October 1998.